

Ph.D. Florence Magnin
Laboratoire EDYTEM
Université de Savoie
F-73376 Le Bourget du Lac cedex
@ florence.magnin@univ-savoie.fr
Author's response to reviewers' reports #2

8th December 2014

Paper title: Thermal characteristics of permafrost in the steep alpine rock walls of the Aiguille du Midi (Mont Blanc Massif, 3842 m a.s.l.)

Authors: F. Magnin, P. Deline, L. Ravel, J. Noetzi, P. Pogliotti

Dear Handling Editor: Dr. Tingjun Zhang, dear reviewers: Dr. Andreas Hasler and anonymous,

Some minor revisions have been performed on this second revised manuscript and all the authors are very grateful to you for having considered our major revisions, for having worked on the improvement of this paper and for having provided additional explanations. We considered every comment of the second revision reports and we hope that our paper now satisfies the required standards for a publication in *The Cryosphere*. However, we had doubts about some comments from A. Hasler as there was a mismatch in between the reviewing report lines and the lines of the uploaded manuscript. Nevertheless, this mismatch was especially confusing at the end of the report and focused on language mistakes. As we worked with a translator for this second revision to make sure that such mistakes didn't occur in the second revised manuscript. Also, some minor corrections have been performed on the English language all along the text.

We increased the legend and axis of the figures as suggested by anonymous reviewers, and you'll find here below the answers to A. Hasler's report.

Our main changes concern the relative weight of the hypothesis on latent heat control and observations on open-fracture effects. We restricted our interpretation on the possible latent heat effects and developed more the description of the fracture effects on the permafrost thermal regime. For that we provided an additional figure (Fig. 8) and modified the abstract and conclusion. Further details on our modifications are provided in the answers to the reports. You'll find a revised version with track changes to clearly distinguish the modifications, and yellow highlights to indicate specific changes that were required and have been done.

Best regards.

Florence Magnin, on behalf of all the co-authors.

Major concerns:

Latent heat:

The dampening of active layer thickness by latent heat consumption is postulated in the revised version as one of the main new findings (abstract, discussion, conclusions 10). This effect is well known in arctic ice-rich soils but I could not see the empirical evidence (zero curtain, isothermal profil) for this effect being relevant in the present data from steep bedrock.

Authors' reply:

Evidences are indeed not clearly presented in a plot and are not as obvious as in arctic soils. So we restricted this part and mentioned it as a future research direction.

Language:

Regarding terms and language the manuscript still needs improvement. Often I had to read the sentences twice to understand. The sentences could be expressed simpler and straighter to the point. There are several mistakes in grammar and style. Terms and adjectives may be used more accurate. Some of them are mentioned in the Detailed comments. The manuscript clearly needs a second revision regarding the language.

Authors' reply:

For this version, we paid a translator.

Non-conductive heat transfer (former section 6.3):

I think to simply erase this content from the manuscript is a petty. I don't agree that doing an analysis as suggested would go beyond the scope of the paper. Making a profile plot of several points in time of BH_N is a minor effort and would allow seeing (qualitatively; see below) where the fracture acts as a heat sink/source and where it simply causes a step in the temperature profile. (The other suggestion with a heat conduction scheme is a larger effort, I agree)

Authors' reply:

Thank you for explaining your thoughts and for providing an example. What we defined as beyond the scope was the heat conduction scheme. Concerning the profile, we totally agree that this is minor effort, and thanks to your explanation, we better understand your expectations. So, we proposed an additional figure to show and discuss the fracture effect following your proposition. This gives more weight to our observations on the fracture and completes the section 6.3. After this revision, the fracture observations have more importance than latent heat hypothesis.

Interannual variability

A large part of the discussion on "Snow cover and micro-meteorological influence" is focused on the interannual variability. Three (of ten) conclusions are made on the interannual variability of the MAGST. Given the small evidence presented (without reference to an illustrative figure) to support of these conclusions this strong focus is not justified.

Authors' reply:

All the points that are discussed are at least visible in Figure 4. Taking into account this comment, we restricted the discussions lines in section 5.3. and gathered our main findings in a single conclusion.

I still have problems with the use of the term "interannual variability": The difference

of 2 years is generalized as interannual variability. Accordingly I can not understand the following answer from the authors to the first review and I don't see how the concerns were considered in the revision:

Reviewer #2: „The term interannual variability of the surface offset needs some explanation for not being confused with interannual variability of the MAGST or MAGT. Interannual variability (or changes) alone is not sufficient in this context. The difference of the means of 2 years should not be called interannual variability. And, can a variability be negative?

Authors' reply: This is true that some explanations would be relevant. In the revised version, interannual variability of SO will be used for data description section (5.1), but in the discussion section (5.3), we explain the meaning of the change in SO in terms of change in MAGST: “On the north face, the higher ASOs at snow-covered sensors (BH_N) compared to at snow-free sensors (N1 and N2) show that the thermo-insulation of snow significantly increases the MAGST. On the south face, the lower ASOs at snow covered sensors (BH_S and S3) compared to snow free conditions (S1 and S2) indicates a lowering of MAGST due to snow.” We agree that the means of 2 years should not be called interannual variability. However, in the submitted version, interannual variability is only described and discussed with annual surface offsets that are not averaged, and concerning the seasonal surface offsets (that are averaged over several seasons) we only describe the spatial pattern.

To make clear what I meant: To compute an interannual variability it needs more than two values (SO or MAGST of more than two years).

Authors' reply:

Ok, so we better understood what you meant. We paid attention to do not use interannual variability for description of change from year-to-year, and we used “interannual changes” instead.

The spatial pattern of interannual SO variability that you postulate on Line 332–350 are based on one single observation (2011 vs. 2012) according to Line 269–273. I agree with your reasoning, that the effect of insulation and reflection on south slopes COULD result in a reduced interannual variability but the presented examples (Line 269ff) do not clearly show this: E.g. why -0.3°C at E1 is considered as larger interannual variability (or better “difference”) whereas $+0.3^{\circ}\text{C}$ at S3 is taken as example for a small variability?

Authors' reply:

The paragraph presents different observations: 1. Snow covered sensors on shaded aspect have greater changes than snow covered sensors on sunny aspect, and the different ranges of changes are illustrated through the comparison of S3 with BH_E and BH_N.

2. Snow covered sensors have opposite change/trend (positive versus negative) than snow free sensors: E1 is here presented to illustrate this opposite change as it has a negative trend, but it is not presented as having a large change!

Possibly, this confusion comes from the language and we paid attention with our translator to make all this section clear.

Why interannual variability of the MAGST appears in the conclusions whereas the results and discussion were mainly on the interannual variability of the SO? This two things are not quite the same because of the variations in MAAT. I don't see this being considered in the text.

Authors' reply:

We use SO to discuss surface temperature. We use ASO to discuss MAGST. Interannual changes of MAGST appear in the conclusions because they are discussed in the manuscript (lines 317 to 323; 339ff of the revised version #1), and the discussion section (5.3) is introduced with the key concepts for interpretation of SO in terms of surface temperature changes (line 296ff).

Also, this is true that MAAT variations have to be taken into consideration before any discussion of changes in ASO. This is why we compare sensors based on the same years of records: e.g. we compare BH_E and BH_N to S3 by using the same years of records for all these sensors (2011 and 2012), because their respective SOs were calculated with the same MAAT, so the changes in MAAT do not influence the different changes in SO from one sensor to another. If we would have compared sensors with different years of record (e.g. compare data of S3 in 2008-2009 and BH_S in 2011-2012), the changes in MAAT between these years would have impacted the results and we would not be able to interpret the part of the change due to changes in MAAT.

Please rephrase Lines 269-277 to clearly express the relevant differences and give a comprehensive overview of the “interannual differences” in a figure to demonstrate an empirical evidence for the spatial pattern that you describe. Otherwise restrict this “hypothesis” to a minimum and avoid to state it as empirical finding of the study in three different conclusions.

Authors reply:

Every pattern described in this paragraph is visible in Figure 4, that was designed to enhance the spatial pattern with the 360° axis. Also, as this is visible in Figure 4, and that the text you refer to only describes the data we have, we do not make any hypothesis, but only data description. But to satisfy this remark, we reformulated and restricted this paragraph, and then, verified the english language with our translator.

Detailed comments:

Line 23: “Analysis ...” Why plural?

Authors' reply:

Sorry, but we did not understand what you meant. “Analysis” is singular. Analyses is plural. So why plural? It was singular in the abstract. After this second revision, we used plural. If your question was “why not plural”, now it is.

Line 24: “,some of them ...” rephrase; “them”?, what of the following is demonstrated the first time?

Authors' reply:

We rephrased.

Line 29ff: reference of second part of the sentence is unclear.

Authors' reply:

We rephrased most of the abstract sentences to make sure that it is a correct english, perfectly understandable and that we clear explain our findings.

Line 30: inhibit? not delay or reduce

Authors reply:

We replaced “inhibit” by “reduce”.

Line 30ff: Consider general comment on “Latent heat”!

Authors reply:

We did, consider our answer to general comment.

Line 76: These scientific goals overlap with the research questions below. Avoid repetition (The precise research questions addressed here are most relevant). Just mention point tree as additional point and why this article may be relevant for it (description of installation and data quality).

Authors reply:

This is important to us to present the goal of our installations. We restricted our presentation of goal (i) and (ii). The goal (iii) makes the transitions with the paper content description.

Line 89–93: Style/grammar: Rephrase questions

Authors reply:

We corrected these questions with our translator.

Line 89 / 92: These two questions could be merged into one.

Authors' reply:

Done.

Line 121: Shift to acknowledgements.

Authors reply:

The authors deeply thought about this demand, but we definitely think that our collaboration and program are better placed in the site description as we do not have any one to acknowledge in these collaborations for this article and that the current work is not supported any more by any of these programs.

Line 205: This local snow accumulation will influence the profiles because the deeper part is influenced by the surrounding snow-free rock.

How much?

Authors reply:

We had trouble to understand this question but we guess that “because” meant “in spite of”. At this level of the article, in the installation description, we are not able to define how much the snow could influence the bedrock temperature at depth, and this question is thus discussed in regard of the data in section 6.3.

Line 230: This is still confusing compared with the statement on Line 218.

The gap is longer but only a part is within the respective year, right?

Authors' reply:

Sorry for this confusion, we reworked the text to make it clear with our translator (in yellow).

Line 231: Why you “felt” so if the effect on the annual mean was so small (see line 228)?

Authors' reply:

The term “felt” is not appropriated. This “feeling” is actually an advice personally communicated from PERMOS people (including some of the co-authors) that usually don't fill gaps > 1.5 months. Then, our gaps > 1.5 months are actually interruptions of several months (e.g. S2 in 2008 has 6 months' gap), so we didn't performed any further tests on such long gaps. Anyway, we rephrased the sentence and explained that these choice was based on the standards of the PERMOS network and were personally communicated.

Line 242: “ASO” is a pleonasm if SO is defined such as on Line 235

Authors reply:

True. So we avoided the repetition in the revised version.

Line 266: At S2 the autumn SSO is larger!

Authors reply:

This may be a confusion, if you look at Figure 4, spring SSO is larger at S2.

Line 294: grammar: “micro-meteorological influences”

Authors reply:

Done.

Line 321ff: (i) is not a cooling effect compared with snow-free rock (but a reduced warming effect compared with thick snow cover). Next sentences need to be adapted accordingly.

Authors reply:

According to us, it is shown as a cooling effect because it is colder than the other sensors in same aspect but in snow free conditions. But, taking into account your point of view, this formulation is also conceivable so we followed your comment.

Line 329: Where is this zero-curtain effect visible? Neither in autumn 2010 nor 2011.

Authors reply:

As described by Hanson and Hoelzle, the zero-curtain-effect is partly ascribed to the effect of melting snow. So, what we see at the surface of BH_S (April 2012), BN_N (July 2011) and S3 (April-May 2012), visible in Figure 5, that we describe as a period of constant temperatures close to 0°C in section 5.2, is what we interpret at zero-curtain-effect in section 5.3, based on literature.

Line 337: grammar: “from one aspect”

Authors reply:

Done.

Line 341: style: “poorly”?

Authors reply:

We rephrased.

Line 363: style: “max. ALT occurred in...”; for BH_S it is problematic to make such a statement due to the missing data

Authors reply:

We reformulated in order to avoid confusions.

Line 389: I can not see how Table 3 supports this statement! MAAT and MART show different evolutions.

Authors reply:

We added an example to show how Table 3 support the fact that $T(z)$ profiles follow MAAT signal.

Line 395–398: Rephrase sentence!

Authors reply:

According to our translator, the sentence was perfectly clear, but it made some minor correction (e.g. turned “deep” into “depth”).

Line 405: temperature gradient can not be correct “-0.2°C/m” ?

Authors reply:

True!! It is been corrected: $-0.02^{\circ}\text{C}\cdot\text{m}^{-1}$

Line 423ff: “In bedrock...”: Sentence contradicts content below! “any specific thickening...”: no thickening? Be precise which study states what!

Authors reply:

We rephrased to avoid such confusions.

Line 433: Daily SO! This is new data that is not shown anywhere! This makes this paragraph not retractable. What is the main message and where can we see that?

Authors reply:

This is true that it is not visible here. This would have involved a specific figure that would have required a long description and introduction of other dataset non presented here (precipitations). We restricted this part of the argumentation, as this is a project for future research, and we rather proposed the effect of summer snow fall as an hypothesis to validate with further investigations to understand the here presented anomaly (reduction of ALT in only one borehole).

Line 442: where can we see the “isothermal conditions”? Compare comment Line 329.

Authors’ reply:

In Figure 6, so we added reference to this figure in the revised version and we extended the sentence to make it clearer.

Line 449: grammar: “temperatures”

Authors’ reply:

Done.

Line 450: grammar: “smoother”

Authors’ reply:

Done

Line 454: Style: What means “usually greater”? Better: “According to a modelling study...”

Authors’ reply:

We modified following this proposition.

Line 456ff: I can not see an empirical evidence for the reasoning presented.

Latter refreezing with larger ALT is a simple result of heat conduction. The freezing in figure 6 BH_S looks quite linear. Detailed data is not presented.

Authors’ reply:

Similarly to the detailed comment on line 433, we restricted this part of the argumentation as this is not a major issue and that will be part of our future research directions.

Line 472: Logic: “MAAT changes up to 10m depth”?

Authors’ reply:

We modified the sentence to avoid such confusion.

Line 473–476: Interesting! Where this is shown?

Authors' reply:

The pattern described (warming above the fracture and cooling below compared to the previous year) is visible in Figure 7, and the coherence of the upper layer with MAAT signal is visible in Table 3. We referred to these figure and table in the second revision.

Line 483: Inflection in the range of measurement error?

Authors' reply:

Yes, so we removed that sentence.

Line 496 and 503: Style: "deep temperatures"? Borehole temperatures?

Authors' reply:

Yes, we replaced with "borehole temperatures"

Line 568: Correct typographical inconsistencies.

Authors' reply:

We reviewed all the bibliography.

Line 600: Gruber AND Haeberli.

Authors' reply:

Done.

Line 757: "depth" instead of "deep",

Authors' reply:

We didn't find where this was referring to, but we corrected our figure captions with our translator in Figure 4 and 5.

Line 761: "depth" instead of "deep", AT is missing in caption

Authors' reply:

We didn't find where this was referring to, but we corrected our figure captions with our translator in Figure 4 and 5.

1 **Thermal characteristics of permafrost in the steep alpine rock**
2 **walls of the Aiguille du Midi (Mont Blanc Massif, 3842 m a.s.l)**

3

4 **F. Magnin¹, P. Deline¹, L. Ravanel¹, J. Noetzli², P. Pogliotti³**

5 [1]{EDYTEM Lab, Université de Savoie, CNRS, Le Bourget-du-Lac, France}

6 [2]{Glaciology and Geomorphodynamics Group, Department of Geography, University of
7 Zurich, Zurich, Switzerland}

8 [3]{ARPA Valle d'Aosta, Saint-Christophe, Italy}

9

10 Correspondence to:

11 F. Magnin (florence.magnin@univ-savoie.fr)

12 P. Deline (philip.deline@univ-savoie.fr)

13 L. Ravanel (ludovic.ravanel@univ-savoie.fr)

14 J. Noetzli (jeannette.noetzli@geo.uzh.ch)

15 P. Pogliotti (paolo.pogliotti@gmail.com)

16 **Abstract**

17 Permafrost and related thermo-hydro-mechanical processes are thought to influence high
18 alpine rock wall stability, but a lack of field measurements means that the characteristics and
19 processes of rock wall permafrost are poorly understood. To help remedy this situation, in
20 2005 work began to install a monitoring system at the Aiguille du Midi (3842 m a.s.l). This
21 paper presents temperature records from nine surface sensors (eight years of records) and
22 three 10-m-deep boreholes (four years of records), installed at locations with different surface
23 and bedrock characteristics. ~~Analysis-In line with of the temperature data confirms~~ previous
24 studies, ~~,our temperature data analyses showed that some of them being demonstrated~~
25 ~~empirically for the first time:~~ micro-meteorology controls the surface temperature, active
26 layer thicknesses are directly related to aspect and ranged from <2 m to nearly 6 m, ~~warm and~~
27 ~~cold permafrost (about -1.5°C to -4.5°C at 10-m-depth) coexists within the Aiguille du Midi,~~
28 ~~resulting in high lateral heat fluxes, and that~~ thin accumulations of snow and open fractures
29 are cooling factors. ~~Thermal profiles empirically demonstrated the coexistence within a single~~
30 ~~rock peak of warm and cold permafrost (about -1.5°C to -4.5°C at 10-m-depth) and the~~
31 ~~resulting lateral heat fluxes.~~ ~~Some observations extent~~ Our results also extended
32 ~~existing current~~ knowledge ~~of the effect of snow, in that is extended~~ we found similar ~~thermo-~~
33 ~~insulation effects as reported for gentle mountain areas. Thick snow warms shaded areas, that~~
34 ~~globally cools the rock surface, and may~~ reduces active layer refreezing in winter and delays
35 its thawing in summer. ~~However, thick snow thermo-insulation has little effect compared to~~
36 ~~the high albedo of snow which leads to cooler conditions at the rock surface in areas exposed~~
37 ~~to the sun.~~ ~~Latent heat consumption due to interstitial water phase changes in bedrock~~
38 ~~discontinuities possibly dampens the active layer and permafrost changes~~ A consistent
39 ~~inflection in the thermal profiles reflected the cooling effect of an open fracture in the~~
40 ~~bedrock, which appeared to~~ act as a thermal cutoff in the sub-surface thermal regime. Our
41 field data are the first to be obtained from an Alpine permafrost site where borehole
42 temperatures are below -4°C, and represent a first step towards the development of strategies
43 to investigate poorly known aspects in steep bedrock permafrost such as the effects of snow
44 cover and fractures.

45

46 **1 Introduction**

47 The last few decades have seen an increase in rockfall activity from steep, high-altitude rock
48 walls in the Mont Blanc Massif (Western European Alps) (Ravanel and Deline, 2010; Deline
49 et al., 2012). Several studies of recent rock avalanches and rockfalls in mid-latitude alpine
50 ranges have ascribed such increases to climate-related permafrost degradation (Deline, 2001;
51 Gruber et al., 2004a; Huggel et al., 2005; Fischer et al., 2006; Huggel et al., 2008; Allen et al.,
52 2009; Ravanel et al., 2010, 2012; Deline et al., 2011). Rockfall magnitude and frequency are
53 thought to be linked to the timing and depth of permafrost degradation, which can range from
54 a seasonal deepening of the active layer to long-term, deep-seated warming in response to a
55 climate signal (Gruber and Haeberli, 2007). Local warming of cold permafrost may be
56 induced by advection and the related erosion of cleft ice (Hasler et al., 2011b), which can lead
57 to unexpected bedrock failures. As Krautblatter et al. (2011) noted, before being able to
58 predict permafrost-related hazards, it is necessary to develop a better understanding of the
59 thermo-hydro-mechanical processes involved, which means collecting rock temperature
60 measurements and developing modeling strategies.

61 Measurement strategies and numerical experiments have been used to investigate the thermal
62 conditions and characteristics of near-vertical and virtually snow-free alpine rock walls that
63 are directly coupled with the atmosphere (Gruber et al., 2003; 2004b, Noetzli et al., 2007).
64 These studies have shown the domination of topographical controls on steep bedrock
65 permafrost distribution, with a typical surface temperature difference of 7-8°C between south
66 and north faces, the possible coexistence of warm and cold permafrost in a single rock mass,
67 and lateral heat fluxes within the rock mass inducing near-vertical isotherms. Hasler et al.
68 (2011a) suggested that, both thin accumulations of snow on micro-reliefs and cleft ventilation
69 may cause deviations of 1°C (shady faces) to 3°C (sunny faces) compared with the smooth,
70 snow-free rock wall model test cases. The thermal influence of snow on steep rock faces has
71 been addressed *via* numerical experiments (Pogliotti, 2011), which have shown that the effect
72 of snow is highly variable and depends on topography, and the depth and timing of the
73 accumulation. However, few empirical data are available to evaluate numerical experiments.
74 Recent advances in the study of steep alpine rock walls have helped to build bridges between
75 what is known about the general characteristics of permafrost and processes related to the
76 microtopography and internal structure of rock masses, which may be significant in their
77 short-term evolution and in permafrost distribution. However, a much larger corpus of field

78 observations and monitoring data for a variety of bedrock conditions is needed to develop,
79 calibrate, and evaluate reliable models.

80 As part of our research into geomorphic activity in the Mont Blanc Massif, in 2005 we started
81 a long-term permafrost-monitoring program at the Aiguille du Midi (AdM), currently the
82 highest instrumented bedrock permafrost site in the European Alps (3842 m a.s.l). This
83 monitoring program was designed to ~~meet three scientific goals:~~

84 characterize ~~the surface temperature of high alpine steep rock walls;~~and

85 determine the thermal state of the permafrost and ~~analyze the variability of~~ active layer ~~and~~
86 ~~deep temperature;~~ and to

87 collect temperature data under variable snow-cover and structural conditions that could be
88 used to calibrate and validate high-resolution numerical experiments on permafrost thermal
89 processes.

90 In this paper we ~~paper addresses goals (i) and (ii). It~~ describe the monitoring program at the
91 AdM, and present temperature data from nine surface mini-loggers and three 10-meter-deep
92 boreholes. Due to the morphology of the AdM, the monitoring network is concentrated in a
93 very small area; however the data obtained allowed us to address the following questions:

94 - How much is of the surface temperature variability over this small area is due to topography
95 ~~in a so small area~~ and snow cover?

96 ~~How much can be the thermal effect of snow cover on surface temperature in steep rock~~
97 ~~walls?~~

98 - How much is of the variability ~~of in the~~ active layer is due to the topography ~~in of the~~ steep
99 rock walls?

100 - What are the thermal effects of snow and fractures on sub-surface temperatures at the AdM?

101 We used eight years of surface records and four years of borehole to analyze seasonal and
102 annual variations in temperature patterns, in the active layer, and in the permafrost thermal
103 regime. We discuss our results in the light of previous research and provide new empirical
104 evidence for the effects of snow and fractures on permafrost in steep rock walls.

105

106 2 Study site

107 The AdM lies on the NW side of the Mont Blanc Massif (Fig. 1). Its summit (45.88° N,
108 6.89°E) consists of three granite peaks (Piton Nord, Piton Central, and Piton Sud) and
109 culminates at 3842 m a.s.l. The steep and partly glaciated north and west faces of the AdM
110 tower more than 1000 m above the Glacier des Pélerins and Glacier des Bossons, while its
111 south face rises just 250 m above the Glacier du Géant (i.e., the accumulation zone of the Mer
112 de Glace). This part of the Mont Blanc Massif is formed by an inclusion-rich, porphyritic
113 granite and is bounded by a wide shear zone. A main, N 40°E fault network intersected by a
114 secondary network determines the distribution of the main granite spurs and gullies (Leloup et
115 al., 2005). The highest parts of the peak tend to be steep, contain few large fractures, and, in
116 places, are characterized by vertical foliation bands and small fissures. The lower parts are
117 less steep and more fractured. In the present paper we use the abbreviation AdM to refer only
118 to the upper section of the Piton Central, between 3740 and 3842 m a.s.l. where most of the
119 instruments are installed. A tourist cable car runs from Chamonix to the Piton Nord. Galleries
120 and an elevator allow visitors to gain the viewing platform on top of the Piton Central, from
121 where there is a 360° panorama of the Mont Blanc Massif.

122 We chose the AdM as a monitoring site for the following scientific and logistical reasons: (i)
123 permafrost is extremely likely due to the AdM's high altitude and the presence of cold-based
124 hanging glaciers on its north face; (ii) the morphology of the peak offers a range of aspects,
125 slope angles, and fracture densities that are representative of many other rock walls in the
126 massif; (iii) the easy access by cable-car from Chamonix and the availability of services (e.g.,
127 electricity) at the summit station. Monitoring equipment was installed as part of the
128 *PERMAdataROC* (2006–2008) and *PermaNET* (2008–2011) projects, funded by the
129 European Union and run jointly by EDYTEM Lab (France), ARPA VdA (Italy), and the
130 Universities of Zurich (Switzerland), Bonn, and Munich (Germany). As such, it complements
131 other rock wall observation sites, for example, those within the Swiss Permafrost Monitoring
132 Network (PERMOS).

133 Data from the monitoring equipment on the AdM was completed by data from ARPA VdA's
134 weather stations, which measured air temperature and relative humidity, incoming and
135 outgoing shortwave and longwave solar radiation, wind speed, and wind direction on the
136 south and north faces between 2006 and 2010. Electrical Resistivity Tomography (ERT) and
137 Induced Polarization (IP) have been measured since 2008 in conjunction with the Universities
138 of Bonn and Munich. High-resolution (cm-scale) triangulated irregular networks (TIN) of

139 rock walls and galleries of the AdM were obtained from terrestrial laser scanning. In July
140 2012, six crack-meters equipped with wireless sensors were installed in major fractures in the
141 Piton Central and Piton Nord in order to complement existing studies of cleft dilatations and
142 shearing movements in rock wall permafrost, to check the stability of the AdM and to test an
143 early warning system. Finally, two GPR surveys were performed along vertical transects in
144 2013 and 2014. Not all of these data were used in the present study but they will contribute to
145 future research.

146

147 **3 Data collection methods**

148 **3.1 Rock temperature monitoring**

149 The present study was based on rock surface temperatures taken at the top of the AdM
150 (between 3815 and 3825 m a.s.l.; Fig. 2) since 2005 by a network of mini-loggers
151 (GeoPrecision PT1000 sensors, accuracy $\pm 0.1^\circ\text{C}$) installed by the University of Zurich and
152 ARPA VdA. Two loggers were installed in snow free locations on each face of the AdM
153 (Table 1). The south face has an additional logger (S3) installed just above a small ledge on
154 which snow accumulates in winter, covering the logger. The loggers record the temperature
155 every hour at depths of 0.03, 0.30, and 0.55 m, in line with the method described by Gruber et
156 al. (2003).

157 In September 2009, three boreholes were drilled in the lower section of the Piton Central, at
158 between 3738 and 3753 m a.s.l.

159 In order to minimize possible thermal disturbances caused by air ventilation in the galleries
160 and heating from staff rooms, the boreholes were drilled several tens of meters below the
161 galleries running through the AdM. The criteria used to decide the exact location of each
162 borehole were the aspect, fracturing, roughness, and angle of the rock wall (Fig. 2). Each
163 borehole was drilled perpendicular to the rock surface and to a depth of 11 meters. Borehole
164 depths were constrained by the drilling equipment and the funding available. The boreholes
165 on the northeast (BH_E) and south (BH_S) faces were drilled in fractured rock walls that
166 slope at 65° and 55° , respectively. Even on rock walls at these angles, snow can accumulate
167 on the micro-reliefs in the face. The borehole on the northwest face (BH_N) was drilled in a
168 vertical, unfractured wall. The only place that snow can accumulate on this wall is on small
169 ledges such as the one above which BH_N was drilled.

170 The boreholes were drilled between September 14th and September 27th, 2009 by a team of
171 five people (two mountain guides, plus three members of the EDYTEM Lab) who had to
172 contend with very variable weather and challenging logistics. For each borehole it was
173 necessary to: (i) install a safety line for the workers, (ii) set up a rope system to carry the
174 equipment from the galleries to the drill site, (iii) install a work platform for the three drillers,
175 (iv) anchor a base on which to fix a rack way, (v) drill the hole using a 380-V Weka
176 Diamond-Core DK 22 electric drill, (vi) insert into the hole a polyethylene PE100 tube (outer
177 diameter: 40 mm; inner diameter: 29 mm) sealed at its bottom, and (vii) remove the work
178 platform. In addition to the difficult environment and harsh weather, the drilling work was
179 complicated by the heterogeneity and hardness of the granite, which took a heavy toll on the
180 equipment (11 diamond heads worn out or broken, a dozen steel tubes damaged, and a motor
181 broken). At first we tried to drill 46-mm-diameter boreholes but we had to increase the
182 diameter to 66 mm so we could use a more robust pipe string. Cooling required 1 to 3 m³ of
183 water per day, which was carried up from Chamonix in 1-m³-tanks via the cable car. Space
184 between the drill hole and the casing was not filled.

185 The three boreholes were fitted with 10-m-long Stump thermistor chains, each with 15-nodes
186 (YSI 44031 sensors, accuracy $\pm 0.1^{\circ}\text{C}$) arranged along a 6-mm fiberglass rod. Following
187 calibration at 0°C in an ice-water basin, the sensors were inserted in BH_S and BH_N in
188 December 2009 and in BH_E in April 2010 (Fig. 3). In order to prevent heat convection, each
189 sensor was separated from the others on the chain by insulating foam. The boreholes were
190 closed at the top, but the chains can be removed to check for thermistor drift. Rock
191 temperatures at depths between 0.3 and 10 m are recorded every three hours (Table 1).
192 Because BH_S is shallower than 10 m, the thermistor chain protrudes from the rock surface
193 by 36 cm. Temperature comparisons between BH_S and BH_N/BH_E were carried out at the
194 closest equivalent depths (*e.g.*, temperatures at a depth of 2.64 m in BH_S were compared
195 with temperatures at a depth of 2.5 m in BH_E and BH_N).

196

197 **3.2 Air temperature and snow cover measurements**

198 In order to aid interpretation of the rock temperature data, we collated air temperature data
199 (AT, Table 1) collected by Météo France at a station 3 m above the top of the Piton Central
200 (3845 m a.s.l.) since 2007. Data prior to 2007 (1989–2006) are very fragmented due to
201 insufficient equipment maintenance and are not used in this study.

202 Two automatic cameras have taken six pictures per day of the south and northeast borehole
203 sites since January 2012. In addition, five graduated stakes were placed around each borehole
204 in order to evaluate the spatial variability of snow accumulation from the photographs. Visual
205 analysis of the photos taken during the winters of 2012 and 2013 showed a thick spatially
206 homogeneous snow cover ($>1\text{m}$), which lasted until late spring at BH_S, and a thin ($<0.5\text{ m}$)
207 spatially variable snow cover at the BH_E, where the rock face is much steeper and more
208 complex (Table 1). Snow accumulations at BH_N and S3 were estimated from field
209 observations. Accumulations of snow at BH_N were restricted to the relatively large ledge
210 above which the borehole is drilled. This snow patch was over 1-m-thick for most of the year.
211 S3 is also frequently covered by $>0.5\text{ m}$ of snow, which accumulates during winter and spring
212 on the small ledge above the sensor. Snow depth is more variable at S3 than at BH_N because
213 the intense solar radiation at S3 leads to more frequent melting.

214

215 **4 Dataset preparation**

216 The borehole time series were all continuous except for short periods for BH_S, as this logger
217 was removed from September 2012 to January 2013 and from October 2013 to January 2014
218 to prevent it being damaged by engineering work close to the borehole. Gaps in the 0.3-m
219 temperature and AT time series were filled in so we could calculate seasonal and annual
220 means (cf. Table 2). First, we calculated daily means from rock temperature time series for
221 days with complete records. Then, we filled short gaps (<5 days) by linear interpolation
222 between the nearest available data points for the same depth. Longer gaps (up to 1.5 month)
223 were filled by replacing missing data with the average value for the 30 days before and 30
224 days after the gap (cf. Hasler et al., 2011a). To fill the longest gaps for E1, N1, S1, and W1
225 (from December 4th, 2007 to February 7th, 2008) we used a third approach that involved
226 applying a linear regression equation, fitted using data from each pair of loggers (e.g., E2 and
227 E1) and records for the missing periods (*i.e.*, December-February) from groups of years with
228 complete records (2006–2007 and 2008–2009). Correlation coefficients for the equations
229 ranged from 0.89 (S1 and S2) to 0.94 (E1 and E2). We tested this approach by simulating
230 corresponding gap periods in the years with complete data and then filling these gaps using
231 the regression equations. Differences between the annual means obtained using this method
232 and the annual means calculated from the complete data set were in the range 0.01–0.15°C
233 and can be considered negligible. Our calculations of seasonal means did not include data
234 | obtained using the 30-day average or linear regression methods. [The longest gap we filled in](#)

235 any one year was <1.5 months, in line with standard practice for the PERMOS network
236 (personal communication). We did not fill gaps longer than 1.5 month per year because we felt
237 that the resulting data would not be reliable enough to give realistic annual means.

238

239 **5 Rock surface temperature**

240 Smith and Riseborough (2002) defined Surface Offset (SO) as the difference between local
241 ~~Mean Annual Air Temperature (MAAT) and Mean Annual Ground Surface Temperature,~~
242 ~~(MAGST).~~ SO is a parameter in the TTOP model (Temperature at the Top of Permafrost,
243 Smith and Riseborough, 1996), originally developed to define the functional relation between
244 air and ground temperatures in polar lowlands and later applied to high-latitude mountainous
245 terrain (Juliussen and Humlum, 2007). SO can be used to quantify the overall effect of ground
246 cover and ground surface parameters on the surface energy balance.

247 We calculated annual SOs (ASO), using Mean Annual Air Temperature (MAAT) means and
248 Mean Annual Ground Surface Temperature (MAGST), and seasonal SOs (SSO) using from
249 seasonal means for winter ~~of rock surface and air temperature of the season for winter~~
250 (December to February), spring (from March to May), summer (from June to August), and
251 fall (from September to November), using time series measured at depths of 0.3-m (boreholes
252 and E2, S2, W2, N2) and 0.1-m (E1, S1, W1, N1) - points we considered representative of
253 surface conditions. We applied a standard lapse rate of $0.006^{\circ}\text{C}\cdot\text{m}^{-1}$ to air temperatures in
254 order to balance the elevation difference between the Météo France station and the sensors.
255 Figure 4 shows ASOs for all the complete years (Fig. 4A), SSOs for snow-free sensors for the
256 available seasons (Fig. 4B), and SSOs for snow-covered sensors for the available seasons
257 (Fig. 4C). We also analyzed daily temperature records for the snow covered sensors and air
258 temperature trends as part of our investigation of the effect of snow cover on snow
259 temperatures (Fig. 5).

260

261 **5.1 Surface Offset patterns**

262 Maximum and minimum ASOs were 9.3°C at S1 in 2011, and 1.3°C at N1 in 2009 (Fig. 4A).
263 These are typical values for the Alps (PERMOS, 2013). On the south face, the snow-covered
264 sensors gave lower values than the snow-free sensors. For example, the ASOs for S3 were
265 between 0.1°C (2010) and 1.4°C (2011) lower than the ASOs for S1. Conversely, on the north

266 side, the snow-covered sensor gave higher ASOs than the snow-free sensors. On a seasonal
267 timescale, the maximum SSOs occurred in summer for the snow-free sensors (Fig. 4B),
268 except for the sensors on the south face (S1 and S2), where the maximum SSOs occurred in
269 spring, with values $>10^{\circ}\text{C}$. The lowest SSOs were recorded in winter, and ranged from
270 approximately 8°C on the south face to $<1^{\circ}\text{C}$ on the north face (N1 and N2). SSO patterns for
271 the snow-covered sensors (Fig. 4C) were opposite to those for the snow-free sensors, except
272 for BH_E. At BH_N and BH_S, SSOs were largest in winter (4.1°C and 9.5°C , respectively)
273 and lowest in summer. At S3, the largest SSO was in the fall. Fall SSOs were also relatively
274 high at BH_N and BH_S. In contrast to SSOs at other snow-covered sensors, SSOs at BH_E
275 followed a similar pattern to that recorded at the snow-free sensors, in that SSO values were
276 directly related to insolation duration.

277 From 2011 to 2012, the changes in ASO at snow-covered and shady sensors such as BH_E
278 and BH_N were greater ($+1.1^{\circ}\text{C}$) than they were at the snow-covered and south-facing
279 sensors (only $+0.3^{\circ}\text{C}$ at S3). Conversely to the snow-covered sensors, the ASO decreased at
280 the snow-free sensors from 2011 to 2012, with, for example, values of -1°C at S2 and -0.3°C
281 at E1. The maximum and minimum ASOs for the different snow-free sensors varied with
282 aspect, with, for example, maximum ASOs in 2008 at W1 and W2, but in 2011 at S1 and S2.

283

284 **5.2 Daily temperatures at snow-covered sensors**

285 Daily temperature curves for the snow-covered sensors are smoothed compared to air
286 temperature oscillation during cold periods (Fig. 5). The S3 and BH_S temperature curves
287 were strongly smoothed from mid-November 2010 to January (BH_S) or April 2011 (gap for
288 S3), and from early December 2011 to mid-May 2012. Both sensors recorded a period of
289 almost constant 0°C conditions from April to mid-May 2012. The temperature curve for
290 BH_N was strongly smoothed until the summer, with a similar constant 0°C period for three
291 weeks in July 2011. Although the BH_E temperature curve from late September to February-
292 March was mostly smoother than daily air temperature curve, the two curves were more
293 closely coupled than they were at the other sensors, as the oscillations in temperatures at
294 BH_E were in-synch with major changes in AT, such as the large drop in temperature in
295 December 2012. From September 2010 to March 2011 and from November 2011 to February
296 2012, the temperatures recorded at BH_E were lower than those recorded at BH_N.

297

298 **5.3 Snow cover and micro-meteorological influences**

299 Normally on steep, snow-free bedrock in the high mountains, the MAGST is higher than
300 MAAT, mainly because of direct solar radiation (Gruber et al. 2004b) but also due to a
301 contribution from reflected solar radiation from large, bright glacier surfaces below
302 measurement points (PERMOS, 2013). In the European Alps, the ASO can be up to 10°C on
303 south-facing rock walls, whereas the maximum ASO values recorded on steep rock walls in
304 Norway are only 3°C, as there is less direct solar radiation at higher latitudes (Hipp et al.,
305 2014). In New Zealand, at similar latitude to the Alps, Allen et al. (2009) reported a
306 maximum ASO value of 6.7°C. This lower value is probably the result of reduced direct solar
307 radiation due to the influence of the oceanic climate and related frequent cloud cover. Most of
308 the surface sensors used in the above studies were installed in snow-free conditions in order to
309 test energy balance models (Gruber et al., 2004b) or for statistical fitting (Allen et al., 2009,
310 Boeckli et al., 2012). At the AdM, the ASO patterns of snow-covered sensors at snow-
311 covered sensors differed from those at snow-free sensors, mainly due to decoupling from
312 atmospheric conditions during the winter season and the lower surface albedo of the snow-
313 free sensors.

314 The differences in ASOs between snow-covered and snow-free sensors on similar aspects
315 show that snow has a substantial effect on the annual energy balance. According to empirical
316 and numerical studies (Hanson and Hoelzle, 2004; Luetsch et al., 2008), snow cover must be
317 at least 0.6-0.8-m-thick to insulate the rock surface from the air temperature, but snow cover
318 on steep rock walls is usually thinner than this insulating threshold (Gruber and Haeberli,
319 2009). The differences between BH_N and BH_E in terms of ASOs and SSOs can probably
320 be ascribed to variations in mean snow cover thickness (Table 1), and demonstrate that the
321 insulating effect of snow can occur locally also in steep rock walls. On the north face, ASOs
322 were higher at snow-covered sensors (BH_N) than at snow-free sensors (N1 and N2),
323 showing that thermo-insulation by snow significantly increases the MAGST. On the south
324 face, ASOs were lower at the snow-covered sensors (BH_S and S3) than at the snow-free
325 sensors (S1 and S2), indicating that snow lowers the MAGST. This reduced warming effect
326 could result from the combination of (i) thin snow cover with negligible thermo-insulation,
327 (ii) a higher surface albedo, (iii) and melt energy consumption (Harris and Corte, 1992;
328 Pogliotti, 2011). The latter two factors seem to be prevalent at the AdM because snow cover
329 on the south face is often greater than 1-m-thick during winter (sect 3.2) leading to a marked
330 smoothing of daily temperature oscillations (Fig. 5). These results extend previous studies on

331 thin snow accumulations (Hasler et al. 2011a). The importance of this **reduced warming** effect
332 on sunny faces is probably reinforced by the fact that snow is present for much of the year at
333 such altitudes, as suggested by (i) the high fall SSOs (early snow accumulation) for snow-
334 covered sensors, (ii) their low summer SSOs, and (iii) by the nearly-constant temperature
335 close to 0°C in late summer (Fig. 5). This constant 0°C temperature may reflect the zero-
336 curtain effect, which results in the snow melting and retards the thawing of the active layer, as
337 has been described for snow-covered gentle mountain slopes (e.g. Hanson and Hoelzle, 2004;
338 Gubler et al., 2011).

339 Different interannual changes were recorded at snow-covered and snow-free sensors. The
340 PERMOS study (2013) has reported analogous differences in interannual variability between
341 rock walls and gentle snow-covered terrain. Interannual changes at the snow-free sensors
342 were mainly related to differences in insolation due to cloud cover. It may be that differences
343 in interannual changes from one aspect to another are also due to variations in cloud
344 formation from year-to-year. Energy balance models have shown that convective cloud
345 formation can cause differences in the spatial distribution of MAGST over a single rock peak
346 (Noetzli et al., 2007). ~~The difference in the spatial distribution of MAGST over a same rock~~
347 ~~peak due to the effect of convective cloud formations was already shown by energy balance~~
348 ~~models (Noetzli et al., 2007), but the evolution of these differences through time with the~~
349 ~~micro-meteorological control was poorly explored.~~ On shady faces, the effect of solar
350 radiation control is greatly reduced and snow cover may be the most important factor
351 affecting interannual changes. Consequently, the temperature at a snow-covered sensor can
352 increase from one year to the next if snow insulation from the atmospheric temperature
353 increases, while the temperature at a snow-free sensor may drop due to reduced insolation. In
354 the case of sun-exposed and snow-covered sensors, such as S3, the balance between warming
355 and cooling effects leads to smaller interannual ASO changes than at sensors in shadier
356 locations, where temperature are mostly controlled by the warming effect of snow insulation.
357 Thus, the influence of snow cover on the surface temperature of high-altitude rock walls is a
358 due to a combination of topography, snow depth, and micro-meteorology.

359

360 **6 Borehole records**

361 Four years of data from the three boreholes allowed us to describe daily temperature patterns
362 (Fig. 6), mean annual Temperature-Depth (T(z)) profiles, and annual temperature envelopes
363 (*i.e.*, the maximum and minimum daily temperatures at each depth in 2011; Fig. 7). We

364 focused on the active layer and the permafrost thermal regime, paying special attention to
365 thermal effects related to snow cover and bedrock structure. We discuss their possible
366 influence on the active layer and bedrock thermal regime.

367

368 **6.1 Active layer**

369 Active Layer Thickness (ALT) varied with aspect, with means of ca. 3 m at BH_E, 5.5 m at
370 BH_S, and 2.2 m at BH_N (Fig. 6). Interannual variability during the monitoring period was
371 ca. 0.7 m for each borehole (Table 3). Maximum ALTs occurred in 2012 at BH_N (2.5 m
372 deep), and in 2013 at BH_E (3.4 m deep), ~~and in 2011 for BH_S (5.9 m deep; however,~~
373 ~~there are no relevant data for 2012).~~ At BH_S, data are missing for 2012 and 2013, but 2010
374 and 2011 data show a maximum ALT in 2011 of 5.9 m.

375 The length of the thawing period, marked by continuous positive temperatures at the
376 uppermost thermistor, also varied according to aspect. It was longest at BH_S, starting in June
377 (April in 2011), but with isolated thawing days already in March (e.g., in 2012). In general,
378 the surface at BH_S refroze in October, but total refreezing of the active layer did not occur
379 until December in 2010 and 2011. The 2011–2012 freezing period was particularly mild and
380 short (3–4 months) at BH_S. This pattern was not as marked at BH_E, which even recorded
381 its lowest surface temperature in 2011–2012. BH_N had the longest freezing periods because
382 temperatures in the rock sub-surface remained positive only from June to October. In 2011,
383 thawing did not start until August. BH_E had the most balanced thawing and freezing periods
384 (ca. 6 months each).

385 The timing of maximum ALT depended on aspect and year (Table 3). In 2010 and 2011,
386 maximum ALT occurred earliest at BH_E, even though the active layer was thicker at BH_E
387 than at BH_N. In 2012 and 2013, BH_N was the first site to reach maximum ALT. In 2010,
388 maximum ALT at BH_S occurred very late, three months after BH_E. Although the BH_S
389 active layer had mostly thawed by mid-July, thawing continued steadily until the end of
390 October. Maximum ALT always occurred later at BH_S than at the other boreholes, but the
391 lowering of the 0°C isotherm was more linear.

392

393 6.2 Thermal regime

394 Annual Temperature-Depth $T(z)$ profiles (Fig. 7A) revealed different thermal regimes. The
395 AdM's Piton Central has both warm (ca. -1.5°C at BH_S) and cold (ca. -4.5°C at BH_N)
396 permafrost (Table 3). Interannual changes were not similar in every borehole. In BH_N and
397 BH_E, the changes over 2010-2013 generally followed the changes in MAAT all along the
398 $T(z)$ profiles. For example, the $T(z)$ profiles show considerable warming from 2010 to 2011 in
399 response to the 2.3°C rise in MAAT (Table 3). The BH_N $T(z)$ profile in 2011 was
400 significantly warmer than in other years for depths up to 2.5 m; however it was colder than
401 2012 for depths greater than 3 m and colder than 2013 for depths greater than 7 m. In BH_S,
402 the mean annual $T(z)$ profile for 2011 showed remarkably high temperature near the surface
403 with positive temperatures up to a depth of 1 m. Temperatures were higher than in 2010 for
404 the shallowest 6 m of the profile but slightly lower than in 2010 below this depth.

405 The zero annual amplitude depth is >10 m for every borehole (Fig. 7B), which is consistent
406 with other bedrock sites in the European Alps (PERMOS, 2007). In 2011, the largest
407 amplitudes in daily temperature (peak to peak) at the surface ($>20^{\circ}\text{C}$) and at 10 m depth
408 (1.6°C) were at BH_E, and the smallest surface (15.5°C) and 10-m (1.0°C) amplitudes were
409 at BH_N and BH_S, respectively. In line with the surface pattern, the minimum $T(z)$ profile
410 from the surface to 1.4-m depth was warmer at BH_N than at the sunnier BH_E (Fig. 7B).

411 The minimum and mean annual $T(z)$ profiles for BH_N contain two distinct sections
412 separated by an inflection at ca. 2.5 m deep (Fig. 7A). This coincides with an 8–10 cm-wide
413 cleft encountered at this depth during the drilling operation. The temperature gradient is
414 negative ($-0.39^{\circ}\text{C m}^{-1}$) from the surface to the cleft, and then positive from the cleft to 10-m-
415 deep (from $0.16^{\circ}\text{C m}^{-1}$ to nearly isothermal). The mean annual profiles for BH_E are almost
416 linear and have a temperature gradient of ca. $-0.02^{\circ}\text{C m}^{-1}$. ~~Small inflections in the profiles~~
417 ~~(e.g., at 1.1 m, 2.5 m, and 7 m depth) occur every year.~~ In the case of BH_S, the upper parts
418 of the annual $T(z)$ profiles for 2010 and 2011 differ greatly, with an almost linear temperature
419 gradient of $-0.07^{\circ}\text{C m}^{-1}$ in 2010, and a much steeper overall temperature gradient of -2.26°C
420 m^{-1} in 2011.

421

422 6.3 Snow cover and bedrock discontinuity controls

423 The coexistence of warm and cold permafrost, and the opposite temperature gradients at
424 BH_S and BH_N, probably due to lateral heat fluxes, are in accordance with the results of
425 numerical simulations (Noetzli et al. 2007).

426 In terms of the permafrost thermal regime, the values recorded at BH_N were below -4°C ,
427 which is a value typical for high latitude monitoring sites, such as those in Svalbard (Noetzli
428 et al., 2014a), and the warmest boreholes of the continuous permafrost zone in Alaska
429 (Romanovsky et al., 2014).

430 The spatial and temporal variability of ALT is consistent with values reported for Swiss
431 boreholes in bedrock (PERMOS, 2013). For example, the thickness and timing of the ALT in
432 BH_E are similar to those recorded at the Matterhorn-Hörnligrat site (3295 m a.s.l, vertical
433 borehole on a crest), with values ranging from 2.89 to 3.66 m between 2008 and 2010, and
434 with maximum ALT occurring between early September and early October. Early studies
435 considered that in bedrock slopes, changes in ALT seem are strongly controlled by summer
436 air temperature, as indicated by the ALT at Schilthorn (2909 m a.s.l) which was twice as thick
437 as usual (from 4-5 m to > 8 m) ~~During the hot summer of 2003 for instance, the ALT at~~
438 ~~Schilthorn (2909 m a.s.l) has been deepened by twice~~, while there was no unusual increase in
439 the ALT under the debris-covered slopes, such as Les Gentianes moraine and the Arolla scree
440 slopes, located in the same area and at similar altitude (PERMOS, 2013).

441 The different patterns of ALT variability at the three AdM boreholes (Table 3) suggest that
442 the air temperature is not the only controlling factor. ~~The thinning of BH_E active layer in~~
443 ~~2011 in contrast with other two boreholes may be ascribed to the cooling effect of a summer~~
444 ~~snow fall, but the cameras and snow probes were not installed yet (sect. 3.2) to check this~~
445 ~~hypothesis. However, a significant drop in daily SO at BH_E occurred just after three~~
446 ~~precipitation episodes (in August, the 26th, and in September, the 3rd-4th and 16th-19th), which~~
447 ~~supports this hypothesis but is hardly visible on a plot. These events occurred just before~~
448 ~~BH_N maximum ALT in 2011 (Table 3). Daily SO generally decreased at BH_S just after the~~
449 ~~precipitation events, and then, rapidly increased. The snow fall would have rapidly melted and~~
450 ~~shortened its cooling effect compared to the more shaded BH_E. BH_N rather showed a~~
451 ~~general increase of its daily SO, which possibly reflects a thermo-insulating effect.~~

452 The relatively mild and short 2011–2012 freezing period at BH_S may have been due to snow
453 insulation, as suggested by the subsequent period of constant temperature from the surface to
454 a depth of 3 m (Fig. 6). This isothermal period coincided with, ~~which may reflect~~ the zero-
455 curtain effect observed at the surface temperature from April to mid-May 2012 (see sections

456 | 5.2 and 5.3, Fig. 5). As reported by Hoelzle et al., (1999), thick, long lasting snow cover
457 | reduces both freezing of the active layer by insulating it from low temperatures and thawing
458 | of the active layer by late snow melting. Such an effect on the active layer freeze-thaw cycles
459 | has been reported by studies in gentle mountain terrains, but has not been observed in steep
460 | bedrock permafrost (Gruber et al. 2004a). A comparison of temperature variations at BH_E
461 | and BH_N clearly shows the effect of snow insulation (Fig. 5). Most notably, winter surface
462 | temperatures are always warmer and smoother at BH_N than at BH_E (Fig. 5) and at depth
463 | (Fig. 7B). Snow appears to have a warming effect at depths of up to 1.4 m. In terms of ALT,
464 | the different trends between BH_E and BH_N during the period 2011-2013 (Table 3) may be
465 | due to the effect of long-lasting snow cover at BH_N modifying its response to the climate
466 | signal. Conversely, the reduced ALT at BH_E in 2011, in contrast with BH_S and BH_N,
467 | may be the result of variations in the effect of summer snow fall on these different faces.
468 | Unfortunately, the cameras and snow stakes that would have allowed us to check this
469 | hypothesis were not installed in 2012 (sect. 3.2). Further studies are needed to verify this
470 | hypothesis.

471 | According to a modelling study, the interannual variability of ALT is greater on sun-exposed
472 | faces, as they respond as much to change in air temperature as to changes in solar radiation
473 | (Gruber et al. 2004a). However, our data did not conform to this prediction, as the change in
474 | ALT at BH_S was similar to the ALTs at the shadier BH_E and BH_N. Furthermore, BH_S
475 | experienced the smallest interannual changes at 10-m-depth, and the shape of its T(z) profiles
476 | between 2010 and 2011 did not follow the trend of the MAAT signal at depths between 6 and
477 | 10 m. This may be due to the consumption of latent heat. In fact, previous studies have
478 | attributed the delaying and dampening effect of latent heat consumption to the thermal
479 | response of bedrock permafrost (Kukkonen et Safanda, 2001; Wegmann et al. 1998, Noetzli
480 | et al. 2007). Field observations during drilling revealed the presence of wet-detritic materials
481 | in the fractures in BH_S, suggesting that latent heat may be consumed by phase changes
482 | between interstitial water and ice during phase-change. ~~This may explain this incoherence.~~
483 | ~~Moreover, the active layer of BH_S shows late-refreezing, especially in its deepest layers that~~
484 | ~~can refreeze a few months after the surface (sect. 6.2, Fig. 6), which is also coherent with~~
485 | ~~latent heat effects. This assumption is supported by previous studies explaining the delaying~~
486 | ~~and dampening effect of latent heat consumption on the thermal response of bedrock~~
487 | ~~permafrost (Kukkonen et Safanda, 2001; Wegmann et al. 1998, Noetzli et al. 2007). BH_S~~
488 | ~~patterns would demonstrate that this process may also be visible at short time scale in steep~~

489 ~~rock walls. The cooling from 2010 to 2011 of its mean annual T(z) profile from 6 to 10-m-~~
490 ~~depth which is inconsistent with the MAAT change (Fig. 7, Table 3) also supports this~~
491 ~~assumption as this likely results of a dampened and delayed response. The probable control of~~
492 ~~latent heat~~ Evidence for latent heat consumption in at BH_S is supported by the temperatures
493 in the borehole, which are around the values required for phase-change processes. Snow
494 accumulation and melting on the south face are an obvious source of water to supply bedrock
495 discontinuities.

496 ~~Interannual changes at~~ Such possible latent heat controls are not visible at BH_E and BH_N
497 ~~followed variations in which interannual changes are coherent with~~ MAAT all along their
498 profiles (except for BH_N in 2011) suggesting that latent heat consumption did not occur
499 changes up to 10-m depth, except for BH_N in 2011 (Fig. 7A). From 2010 to 2011 ~~t~~The
500 BH_N T(z) profile ~~The significant~~ warmed significantly above the cold inflection-. This in
501 coherence with ~~followed~~ MAAT ~~change from 2010 to 2011~~ (Table 3), but the colder
502 conditions below the inflection ~~has no~~ were not in accordance ~~coherence~~ with the climate
503 signal. Hence, the fracture seems to act as a thermal cutoff between the surface layer and the
504 deep bedrock. The sharp inflection in the profiles at the fracture depth, which is especially
505 prominent in the mean and minimum annual T(z) profiles, indicates that the fracture locally
506 cools the rock. Mean annual temperature is even lower at depth of 2.5 m than it is at the
507 surface, which, as explained above, is probably insulated by the snow cover. Seasonal
508 temperature profiles for BH N (Fig. 8) show a relatively large difference between the
509 temperature gradient above and below the fracture depth during winter (Dec. to Feb.) and a
510 much smaller difference during summer (June to Aug.). In winter, the temperature gradient
511 above the fracture depth was quite low (between 0.5 and 0.9°C m⁻¹ between 0.3 and 2.5 m,
512 depending on the year), but much higher at greater depth (between 5.1 and 6°C m⁻¹ between
513 2.5 and 3 m, 6.3°C m⁻¹ between 3 and 4 m, and >4°C.m⁻¹ down to 7 m). In summer the
514 difference in temperature gradients was much less marked, although there was still a
515 substantial change in temperature gradient at the fracture depth. The mean gradient stepped up
516 from between -1.4°C and -2°C m⁻¹ between 0.3 to 2-m-depth, to between ~~the fracture depth~~
517 with a step in the ~~-2.3 to -5.1°C m⁻¹ between 2 and 2.5-m-depth.~~ The temperature gradient
518 remained relatively high (> 2.4°C.m⁻¹ except in 2010) up to 4-m-depth, and then progressively
519 decreased. These observations suggest that the fracture provokes a heat sink, with greater
520 downward propagation in winter, and a more localized effect in summer. This cooling effect
521 may be due to air ventilating through the open fracture, a process that has been shown to have

522 an important cooling effect on steep rock wall permafrost (Hasler et al. 2011a). In our study
523 this cooling effect was greater when the air temperature was low. Nevertheless, despite this
524 this cooling effect, water percolation can occur along the fracture and heat advection could
525 locally warm the rock (Hasler et al. 2011b). However, the temperature data for BH_N do not
526 provide any evidence for this. ~~The small inflections visible in~~The temperature profile for
527 BH_E ~~at several depths every year (sect. 6.2) are also possibly induced by bedrock~~
528 ~~discontinuities, but they have a negligible impact on~~is generally linear indicating that
529 conduction is the dominant heat transfer process (Williams and Smith, 1989). ~~The fracture~~
530 ~~width is probably the critical factor controlling the magnitude of the perturbation.~~Thus, active
531 layer thickness and timing and permafrost temperatures at the AdM are controlled by a
532 number of factors that interact with each other, including snow cover, latent heat consumption
533 (which delays and dampens short-term responses to climate signals), and cooling effect due to
534 air ventilation within open fractures.

535

536 7 Conclusion

537 The high altitude, morphology, and accessibility of AdM make it an exceptional site for
538 investigating permafrost in steep rock walls. A monitoring network installed on the AdM to
539 investigate the thermal effects of topography, snow cover and fractures on permafrost
540 provided eight years of rock surface temperature and four years of **borehole** temperature data.
541 The results of our analyses of this new dataset supported the findings of previous field studies
542 and a number of numerical experiments:

- 543 - The thermal characteristics of the AdM's rock walls are typical of steep bedrock
544 permafrost. The spatial variability of surface temperature, active layer thickness
545 and timing, and the permafrost thermal regime are mainly controlled by
546 topography.
- 547 - **Borehole** temperature data confirm the characteristics of the sub-surface thermal
548 regime predicted by numerical experiments, in particular the coexistence within a
549 single rock peak of warm and cold permafrost, which generates lateral heat fluxes
550 from warm to cold faces.

551 —~~MAGST are not uniform at all aspects around a single rock peak~~ is controlled by
552 micro-meteorological parameters (variable cloud formation from year-to-year)
553 when the rock face is in snow free conditions, and by local accumulations where
554 there is snow on the face. Snow-free areas and snow-covered areas can show
555 opposite trends. This may be ascribed to variable cloud formation from year to
556 year.

557
558
559
560
561
562
563
564
565
566
567
568
569
570
571
572
573
574
575
576
577
578
579
580
581
582
583
584
585
586
587
588
589
590
591
592
593

- ~~-~~
 - ~~■ Interannual change of snow-covered sensors may be opposite to snow-free sensors as the snow can increase the MAGST due to higher thermo-insulation (more precipitations) meanwhile MAGST at snow-free sensors can decrease because of reduced solar radiation and lower air temperature.~~
 - Surface temperature data confirm that thin (not-insulating) snow cover can lower the MAGST surface temperature because of a due to the low snow surface albedo ~~strong reduction of surface albedo.~~
 - ~~1. Open fractures have a strong, localized cooling effect possibly resulting from air ventilation within the fracture.~~
- Our results also extended Observations the results from of previous studies ~~are extended and new characteristics are highlighted:~~
- Sensors with thick snow cover showed evidence of a similar thermo-insulation effect to that found on gentle mountain slopes, with smoothing of daily temperatures in winter, a melting period marked by constant surface temperature of around 0°C, reduced freezing of the active layer in winter, and delayed thawing of the active layer in summer.
 - Thick snow accumulations warm MAGST of shady areas and increases interannual changes compared with sunny areas which are cooled by snow blocking solar radiation, and where interannual changes are reduced by the balance between the opposite effects of thermo-insulation and strong albedo.
 - ~~— the cool the MAGST of sun-exposed sensors. On south faces, a thick (insulating) snow cover may cool the MAGST because of a prevailing effect of increased surface albedo and latent heat consumption. On north faces, thermo-insulation can dominate and snow can warm MAGST similarly to gentle mountain slopes.~~
 - ~~— The interannual changes of MAGST in snow-covered areas are greater on shaded aspects than on sunny faces because the latter combines the controls of solar radiation and snow.~~
 - ~~— The effects of snow cover on ALT in steep rock walls follow the same rules of gentle morphologies. In particular: (i) a thick (insulating) snow cover may reduce cooling during winter leading to a thickening of ALT; (ii) a long-lasting (early summer) snow cover may reduce summer warming leading to a thinning of ALT. Such a contrasting effects may coexist or not both in space (e.g. aspects) and time (e.g. season).~~
 - Open fractures have a strong, localized cooling effect, possibly due to air ventilation within the fracture. This cooling effect is greater in winter and the heat sink mainly affects the 3-4 m below the fracture.

594 | ~~1. Latent heat due to phase change processes of interstitial water in bedrock fractures can~~
595 | ~~dampen active layer and permafrost interannual changes in steep bedrock.~~

596

597 **8. Further developments**

598 The thermal characteristics of the AdM illustrate the complexity of the processes controlling
599 the thermal regime of shallow layers in rock wall permafrost. Modelling these processes
600 represents a major challenge but the data presented here provide a step towards achieving this
601 goal. Studies into the controlling effect of snow cover are needed in order to determine the
602 impact of thick accumulations and summer snow fall on ALT and permafrost changes. The
603 current research project has already collected a large amount of data, including picture
604 showing the evolution of the south and northeast faces of the AdM, snow-stake
605 measurements, and borehole records. Further analyses of these data would help improve
606 understanding of rock fall activity. Research into latent heat consumption in compact bedrock
607 may also provide insight into ALT thickness and timing on some snow-covered rock walls,
608 and into permafrost evolution over short-time scales. The BH_N fracture could be used to
609 investigate non-conductive heat transfers, for example by developing a heat conduction
610 scheme. Ground-penetrating radar measurements of the northwest face, including BH_N,
611 offer a detailed picture of the bedrock discontinuities and provide useful additional data for
612 developing a heat flow model integrating bedrock structure. The combined use of crack-
613 meters, air temperature measurements, and borehole data provides a promising avenue for
614 developing understanding of the thermal and mechanical factors affecting rock wall
615 instabilities.

616 The dataset presented here was used for evaluation of statistical and numerical models
617 designed to map the distribution of permafrost in the Mont Blanc Massif (Magnin et al., 2014)
618 and to predict the distribution and evolution of the temperature field at the AdM over the next
619 century (Noetzli et al., 2014b). The statistical model will be used to determine bedrock
620 temperatures and the related permafrost thermal regime at rock fall locations in order to
621 analyze the relationship between bedrock temperature and rock failures.

622

623 *Acknowledgements:* We would like to thank S. Gruber, U. Morra di Cella, E. Cremonese, and
624 E. Malet, for their help with equipment installation and data acquisition at the Aiguille du
625 Midi. The Chamonix *Compagnie des Guides* provided invaluable assistance with the drilling
626 operations. We would also like to thank the *Compagnie du Mont Blanc* (especially E.

627 Desvaux) for allowing access to the site, and Météo France for providing air temperature data.
628 Thank you to A. Hasler and anonymous reviewer for their useful comments and
629 recommendations. The english text was corrected by P. Henderson. This work was supported
630 by the Region Rhône-Alpes (*CIBLE* program).

631 **References**

632

633 Allen, S. K., Gruber, S., and Owens, I. F.: Exploring steep bedrock permafrost and its
634 relationship with recent slope failures in the Southern Alps of New Zealand, *Permafrost*
635 *Periglac.*, 20, 345–356, doi:10.1002/ppp.658, 2009.

636

637 Boeckli, L., Brenning, A., Gruber, S., and Noetzli, J. Permafrost distribution in the European
638 Alps: calculation and evaluation of an index map and summary statistics. *The Cryosphere*
639 *Discuss.*, 6, 849–891, doi:10.5194/tcd-6-849-2012, 2012.

640

641 Deline, P.: Recent Brenva rock avalanches (Valley of Aosta): new chapter in an old story?
642 *Supplementi di Geografia Fisica e Dinamica Quaternaria*, 5, 55–63, 2001.

643

644 Deline, P., Alberto, W., Broccolato, M., Hungr, O., Noetzli, J., Ravanel, L., and Tamburini,
645 A.: The December 2008 Crammont rock avalanche, Mont Blanc massif area, Italy, *Nat.*
646 *Hazard Earth Sys.*, 11, 3307–3318, 2011.

647

648 Deline, P., Gardent, M., Magnin F., and Ravanel, L.: The morphodynamics of the Mont Blanc
649 massif in a changing cryosphere: a comprehensive review, *Geogr. Ann. A*, 94(2), 265–283,
650 2012.

651

652 Fischer, L., Käab, A., Huggel, C., and Noetzli, J.: Geology, glacier changes, permafrost and
653 related slope instabilities in a high-mountain rock wall: Monte Rosa east face, Italian Alps,
654 *Nat. Hazard Earth Sys.*, 6, 761–772, 2006.

655

656 Gruber, S. and Haeberli, W.: Permafrost in steep bedrock slopes and its temperature related
657 destabilization following climate change, *J. Geophys. Res-Earth.*, 112, F02S13,
658 doi:10.1029/2006JF000547, 2007.

659

660 Gruber S. and Haeberli W.: Mountain permafrost, in: *Permafrost soils*, Margesin R, Springer,
661 16, 33-44, 2009.

662

663 Gruber, S., Peter, M., Hoelzle, M., Woodhatch, I., and Haeberli, W.: Surface temperatures in
664 steep alpine rock faces: a strategy for regional-scale measurement and modelling, in:
665 *Proceedings of the 8th International Conference on Permafrost*, L. Arenson, Zürich, 325-330,
666 2003.

667

668 Gruber, S., Hoelzle, M., and Haeberli, W.: Permafrost thaw and destabilization of Alpine rock
669 walls in the hot summer of 2003, *Geophys. Res. Lett.*, 31, L13504,
670 doi:10.1029/2004GL0250051, 2004a.

671

672 Gruber, S., Hoelzle, M., and Haeberli, W.: Rock-wall temperatures in the Alps: modelling
673 their topographic distribution and regional differences, *Permafrost Periglac.*, 15, 299–307,
674 doi: 10.1002/ppp.501, 2004b.

675

676 Gubler, S., Fiddes, J., Keller, M., and Gruber, S.: Scale-dependent measurement and analysis
677 of ground surface temperature variability in alpine terrain, *The Cryosphere*, 5, 431–443, 2011.

678

679 Hanson, S. and Hoelzle, M.: The thermal regime of the active layer at the Murtèl rock glacier
680 based on data from 2002. *Permafrost Periglac.*, 15, 273–282, doi: 10.1002/ppp.499, 2004.

681

682 Harris, S. and Corte, A.: Interactions and relations between mountain permafrost,
683 glaciers, snow and water, *Permafrost Periglac.*, 3, 103–110, 1992.

684

685 Hasler, A., Gruber, S., and Haeberli, W.: Temperature variability and offset in steep alpine
686 rock and ice faces, *The Cryosphere*, 5, 977–988, doi:10.5194/tc-5-977-2011, 2011a.

687

688 Hasler, A., Gruber, S., Font, M., and Dubois, A.: Advective heat transport in frozen rock
689 clefts - conceptual model, laboratory experiments and numerical simulation. *Permafrost*
690 *Periglac.*, 22, 378–349, doi: 10.1002/ppp.737, 2011b.

691

692 Hipp, T., Etzelmüller, B. and Westermann, S.: Permafrost in Alpine Rock Faces from
693 Jotunheimen and Hurrungane, Southern Norway. *Permafrost Periglac.*, 25: 1–13.
694 doi: 10.1002/ppp.1799, 2014.

695

696 Hoelzle, M., Wegmann, M., and Krummenacher, B.: Miniature temperature dataloggers for
697 mapping and monitoring of permafrost in high mountain areas: first experience from the
698 Swiss Alps. *Permafrost Periglac.*, 10: 113–124. doi: 10.1002/(SICI)1099-
699 1530(199904/06)10:2<113::AID-PPP317>3.0.CO;2-A, 1999.

700

701 Huggel, C., Caplan-Auerbach, J., and Wessels, R.: Recent extreme avalanches triggered by
702 climate change, *EOS, Transactions American Geophysical Union*, 89, 469–470, 2008.

703

704 Huggel, C., Zraggen-Oswald, S., Haeberli, W., Kääh, A., Polkvoj, A., Galushkin, I., and
705 Evans, S.G.: The 2002 rock/ice avalanche at Kolka/Karmadon, Russian Caucasus: assessment
706 of extraordinary avalanche formation and mobility, and application of Quick- Bird satellite
707 imagery, *Nat. Hazard Earth Sys.*, 5, 173–187, doi:10.5194/nhess-5-173-2005, 2005.

708

709 Krautblatter, M., Huggel, C., Deline, P., and Hasler, A.: Research Perspectives on Unstable
710 High-alpine Bedrock Permafrost: Measurement, Modelling and Process Understanding.
711 *Permafrost Periglac.*, 23, 80–88, DOI: 10.1002/ppp.740 2011.

712

713 Juliussen, H. and Humlum, O.: Towards a TTOP ground temperature model for mountainous
714 terrain in central-eastern Norway. *Permafrost Periglac.*, 18, 161–184, doi: 10.1002/ppp.586,
715 2007.

716

717 Kukkonen, I. T. and J. Safanda.: Numerical modelling of permafrost in bedrock in northern
718 Fennoscandia during the Holocene, *Global Planet. Change*, 29, 259– 273, 2001.

719

720 Leloup, P. H., Arnaud, N., Sobel, E. R., and Lacassin, R.: Alpine thermal and structural
721 evolution of the highest external crystalline massif: The Mont Blanc. *Tectonics*, 24, TC4002,
722 doi: 10.1029/2004TC001676, 2005.

723

724 Le Roy, M.: Reconstitution des fluctuations glaciaires holocènes dans les Alpes occidentales,
725 Thèse de Doctorat de Géographie, Université de Savoie, Le Bourget du Lac, 344 pp, 2012.

726

727 Luetschg, M., Lehning, M., and Haeberli, W.: A sensitivity study of factors influencing
728 warm/thin permafrost in the Swiss Alps, *J. Glaciol.*, 54, 696–704, 2008.

729

730 Magnin, F., Brenning, A., Bodin, X., Deline, P., Ravanel, L.: Statistical modelling of rock
731 wall permafrost distribution: application to the Mont Blanc massif, *Géomorphologie*,
732 Manuscript submitted.

733

734 Noetzli, J., Gruber, S., Kohl, T., Salzmann, N., and Haeberli, W.: Three-dimensional
735 distribution and evolution of permafrost temperatures in idealized high-mountain topography,
736 *J. Geophys. Res-Earth*, 112, F02S13, doi:10.1029/2006JF000545, 2007.

737

738 Noetzli, J., Christiansen, H. H., Guglielmin, M., Romanovsky, V. E., Shiklomanov, N. I.,
739 Smith, A.L., and Zhao, L.: Permafrost thermal state, in: *State of the Climate in 2013*, *Bull.*
740 *Amer. Meteor. Soc.*, 95, 2014a.

741

742 Noetzli, J., Ravanel L., and Deline P.: Combining measurements and modelling to describe
743 the permafrost conditions at the Aiguille du Midi (3842 m asl, Mont Blanc Massif). *The*
744 *Cryosphere*, in preparation.

745

746 PERMOS: Permafrost in Switzerland 2002/2003 and 2003/2004, in: Vonder Mühll, D. (eds.),
747 *Glaciological Report (Permafrost) No. 4/5 of the Cryospheric Commission of the Swiss*
748 *Academy of Sciences, Zürich*, 121 pp, 2007.

749

750 PERMOS: Permafrost in Switzerland 2008/2009 and 2009/2010, in: Noetzli, J. (eds.),
751 *Glaciological Report (Permafrost) No. 10/11 of the Cryospheric Commission of the Swiss*
752 *Academy of Sciences, Zürich*, 95 pp, 2013.

753

754 Pogliotti, P.: Influence of Snow Cover on MAGST over Complex Morphologies in Mountain
755 Permafrost Regions. PhD thesis, Turin, Italy, Università degli Studi di Torino, 79 pp, 2011.

756

757 Ravanel, L. and Deline P.: Climate influence on rockfalls in high-Alpine steep rock walls: the
758 north side of the Aiguilles de Chamonix (Mont Blanc massif) since the end of the ‘Little Ice
759 Age’, *The Holocene*, 21, 357–365, doi: 10.1177/0959683610374887, 2010.

760

761 Ravanel, L., Allignol, F., Deline, P., Gruber, S., and Ravello, M.: Rock falls in the Mont
762 Blanc Massif in 2007 and 2008, *Landslides*, 7, 493–501, 2010.

763

- 764 Ravanel, L., Deline, P., Lambiel, C., and Vincent C.: Intability of a high Alpine rock ridge:
765 the lower Arête des Cosmiques, Mont Blanc massif, France, *Geogr. Ann. A*, 95, 51–66, doi:
766 10.1111/geoa.12000, 2012.
- 767
- 768 Romanovsky, V. E., Smith, S. L., Christiansen, H. H., Shiklomanov, N. I., Streletskiy, G. A.,
769 Drozdov, D. S., Malkova, G. V., Oberman, N. G., Kholodov, A. L., and Marchenko, S. S.:
770 [Terrestrial permafrost, in: *State of the Climate in 2013*, *Bull. Amer. Meteor. Soc.*, 95, S139–
771 S141, 2014.
- 772
- 773 Smith, M. W. and Riseborough, D. W.: Permafrost monitoring and detection of climate
774 change. *Permafrost Periglac.*, 7, 301–309, doi: 10.1002/(SICI)1099-
775 1530(199610)7:4<301::AID-PPP231>3.0.CO;2-R, 1996.
- 776
- 777 Smith, M. W. and Riseborough, D. W.: Climate and the limits of permafrost: a zonal analysis.
778 *Permafrost Periglac.*, 13, 1–15, doi: 10.1002/ppp.410, 2002.
- 779
- 780 Williams, P. J. and Smith, M. W.: *The frozen earth*, *Studies in polar research*, Cambridge
781 University Press, Cambridge, 306 pp., 1989.

782 **Tables**

783

Site Code	Elevation [m a.s.l.]	Aspect [°]	Slope [°]	Sensor depths [m]	Estimated snow accumulation [m]
BH_S	3753	135	55	0.14, 0.34, 0.74, 1.04, 1.34, 1.64, 2.14, 2.64, 3.64, 4.64, 6.64, 8.64, 9.64	> 0.8
BH_N	3738	345	90	0.3, 0.5, 0.7, 0.9, 1.1, 1.4, 1.7, 2, 2.5, 3, 4, 5, 7, 9, 10	> 1.0
BH_E	3745	50	65	0.3, 0.5, 0.7, 0.9, 1.1, 1.4, 1.7, 2, 2.5, 3, 4, 5, 7, 9, 10	< 0.6
W1	3825	270	80	0.1	0
S1	3820	140	74	0.1	0
N1	3820	354	84	0.1	0
E1	3823	124	60	0.1	0
N2	3820	334	80	0.03, 0.1, 0.3, 0.55	0
E2	3820	118	60	0.03, 0.1, 0.3, 0.55	0
S2	3815	160	85	0.03, 0.1, 0.3, 0.55	0
W2	3825	270	85	0.03, 0.1, 0.3, 0.55	0
S3	3820	158	70	0.03, 0.1, 0.3, 0.55	0.5 to 1.0
AT	3845	0	0		0

784 **Table 1.** Instrument positions.

785 BH: borehole thermistor chains, X1 and X2: rock surface temperature loggers, AT: air
786 temperature. Estimated snow accumulation: from automatic cameras and probes for BH_S
787 and BH_E (winter 2012 and 2013), from field observation for S3 and BH_N.

Year	2006				2007				2008				2009				2010				2011				2012				2013			
Season	Wi	Sp	Su	Fa	Wi	Sp	Su	Fa	Wi	Sp	Su	Fa	Wi	Sp	Su	Fa	Wi	Sp	Su	Fa	Wi	Sp	Su	Fa	Wi	Sp	Su	Fa	Wi	Sp	Su	Fa
N1	[Dark Blue]																[Light Blue]															
E1	[Dark Blue]																[Light Blue]															
S1	[Dark Blue]																[Light Blue]															
W1	[Dark Blue]																[Light Blue]															
N2	[Dark Blue]				[Dark Blue]				[Dark Blue]				[Dark Blue]				[Dark Blue]				[Dark Blue]				[Dark Blue]							
E2	[Dark Blue]				[Dark Blue]				[Dark Blue]				[Dark Blue]				[Dark Blue]				[Dark Blue]				[Dark Blue]							
S2	[Dark Blue]				[Dark Blue]				[Dark Blue]				[Dark Blue]				[Dark Blue]				[Dark Blue]				[Dark Blue]							
W2	[Dark Blue]				[Dark Blue]				[Dark Blue]				[Dark Blue]				[Dark Blue]				[Dark Blue]				[Dark Blue]							
S3	[Dark Blue]				[Dark Blue]				[Dark Blue]				[Dark Blue]				[Dark Blue]				[Dark Blue]				[Dark Blue]							
BH_S	[Dark Blue]																[Light Blue]															
BH_E	[Dark Blue]																[Light Blue]															
BH_N	[Dark Blue]																[Light Blue]															
AT	[Dark Blue]																[Light Blue]															

789 **Table 2.** Data availability after gap filling.

790 **Wi:** December, January, February; **Sp:** March, April, May; **Su:** June, July, August; **Fa:**
 791 September, October, November.

792 Red sections indicate where gaps <1.5 month per year have been filled in order to calculate
 793 annual means but seasonal means were not calculated for the seasons in question. The time
 794 series interrupted with white gap areas indicate that annual mean is not computed for the
 795 concerned year.

Year	BH_E			BH_S			BH_N			MAAT
	ALT [m]	Max. ALT [dd.mm]	MART _{10m} [°C]	ALT [m]	Max. ALT [dd.mm]	MART _{10m} [°C]	ALT [m]	Max. ALT [dd.mm]	MART _{10m} [°C]	
2010	3.1	27.07	-	5.2	23.10	-1.4	1.8	28.08	-4.7	-9
2011	2.7	30.08	-3.8	5.9	22.10	-1.5	2.3	18.09	-4.6	-6.7
2012	3.3	26.08	-3.6	-	-	-	2.5	26.08	-4.3	-7.7
2013	3.4	08.09	-3.6	5.8	30.09	-	2.2	25.08	-4.5	-

796 **Table 3.** Borehole and air temperature records.

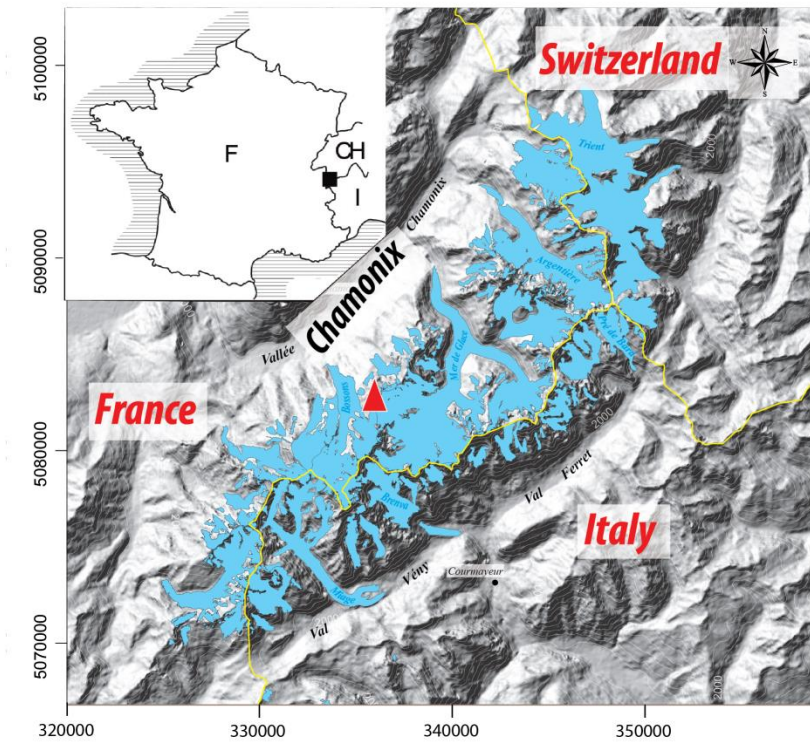
797 ALT: Active Layer Thickness

798 MART_{10m}: Mean Annual Rock Temperature at 10-m depth

799 MAAT: Mean Annual Air Temperature

800

801 **Figures**



802

803

804 **Figure 1.** Location of the Mont Blanc Massif and the Aiguille du Midi (red triangle)
805 (modified from Le Roy, 2012).

806

807

808

809

810

811

812

813

814

815

816

817



818

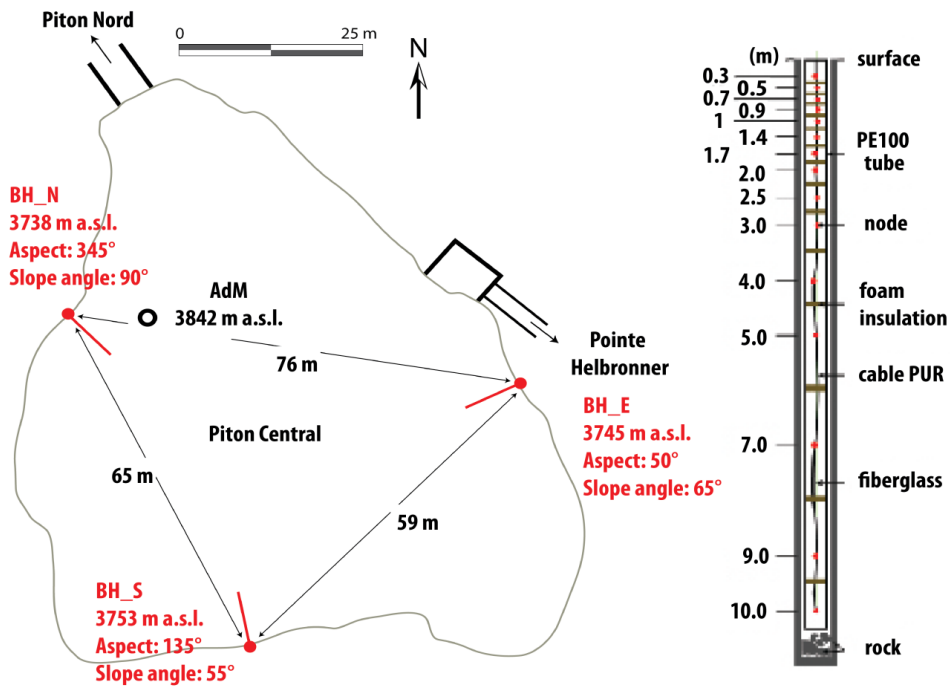
819

820 **Figure 2.** The Aiguille du Midi with snow camera, air temperature, rock surface temperature,
 821 and borehole logger locations.

822 *Pictures: S. Gruber (top left and right, bottom left); P. Deline (bottom right).*

823

824



825

826

827

828 **Figure 3.** Borehole positions and components.

829 Left: Horizontal cross-section through the AdM's Piton Central. Borehole positions are
830 marked in red.

831 Right: 10-m-long, 15-node thermistor chain installed in the boreholes.

832

833

834

835

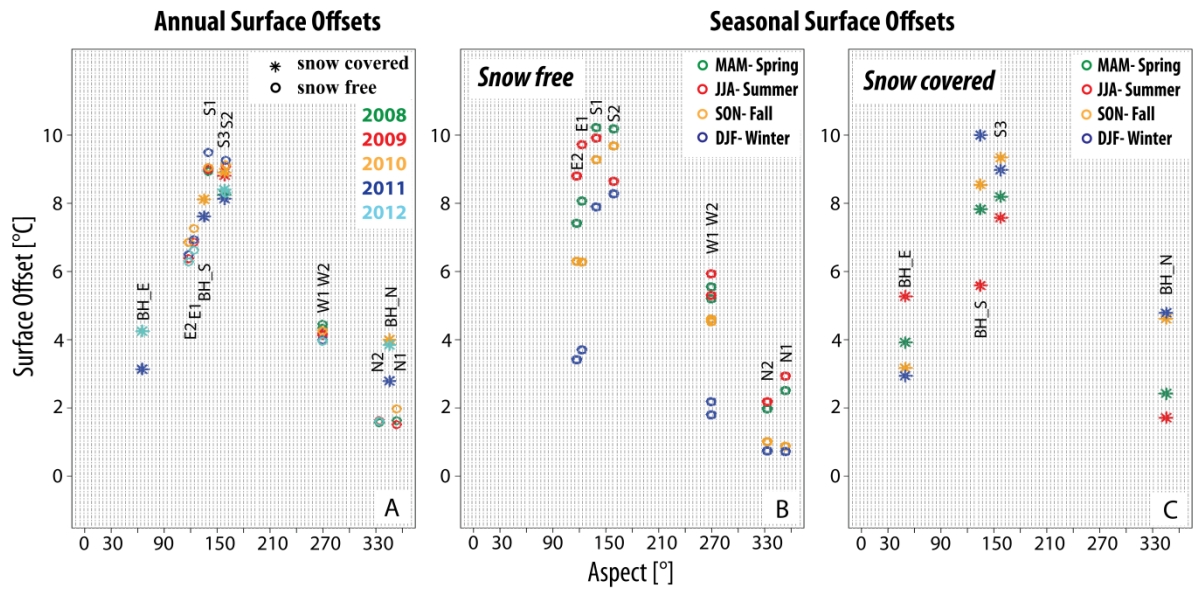
836

837

838

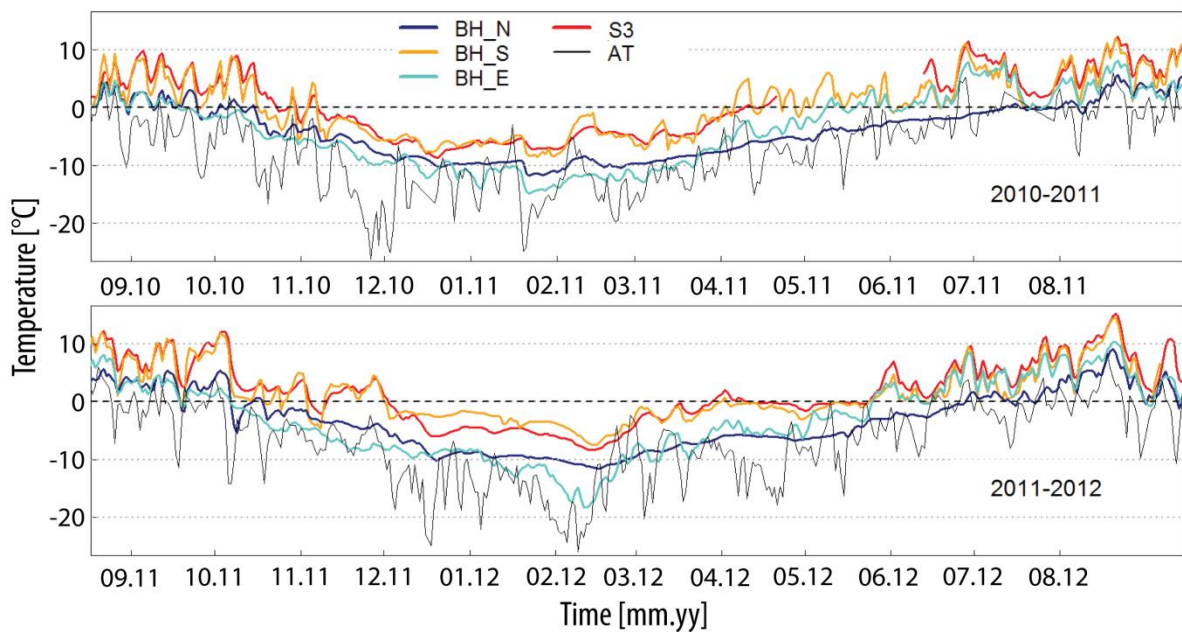
839

840

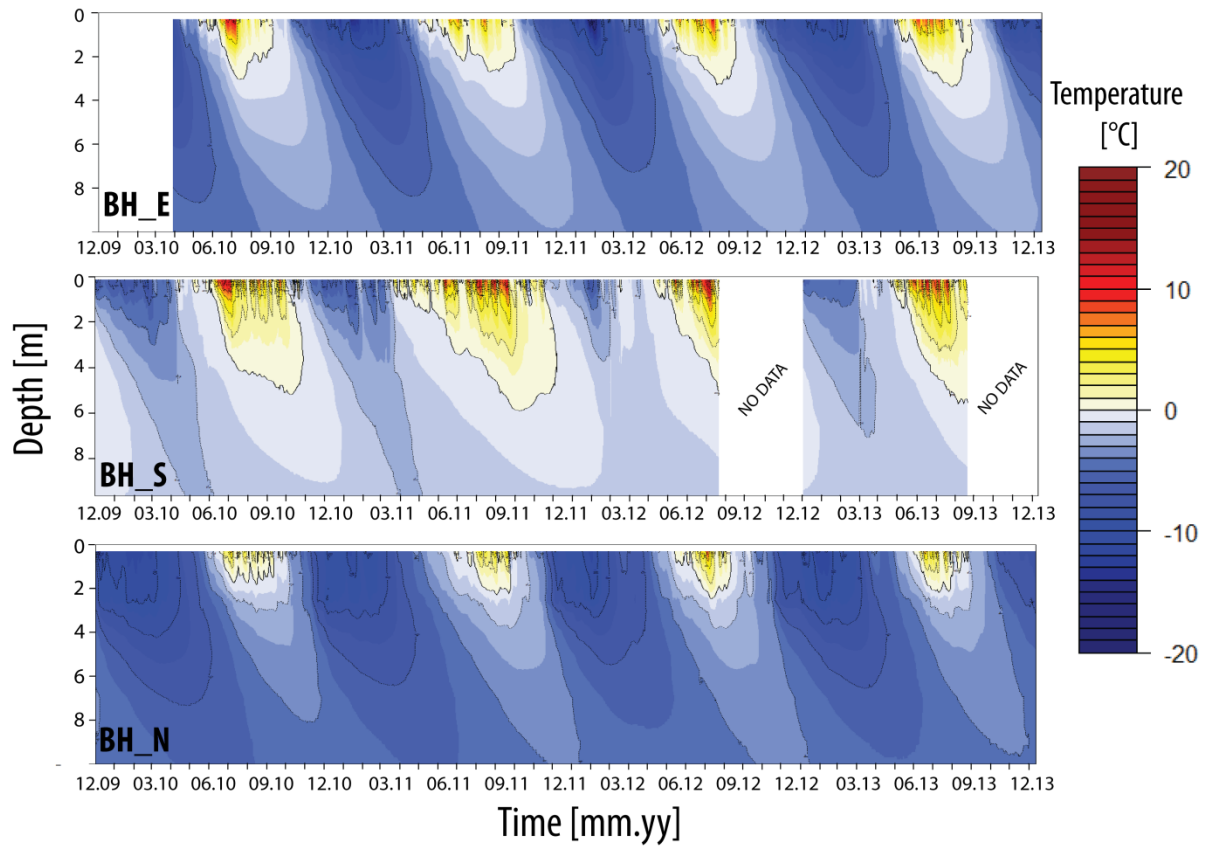


841
 842 **Figure 4.** Annual and Seasonal Surface Offsets calculated from sensors at 0.3-m **depth**.
 843 ASOs are shown for all the available years. SSOs are the mean values for the available
 844 seasons for each logger listed in Table 2.

845



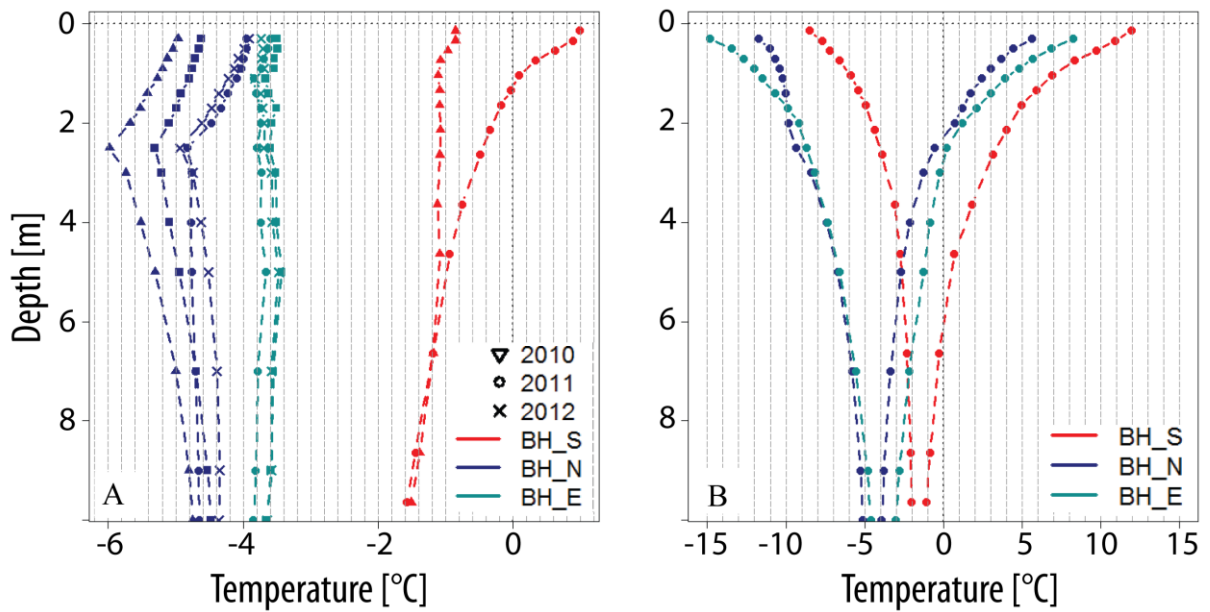
846
 847 **Figure 5.** Daily temperature records at 0.3-m **depth** for snow-covered sensors for the 2010-
 848 2011 and 2011-2012 hydrological years.



849

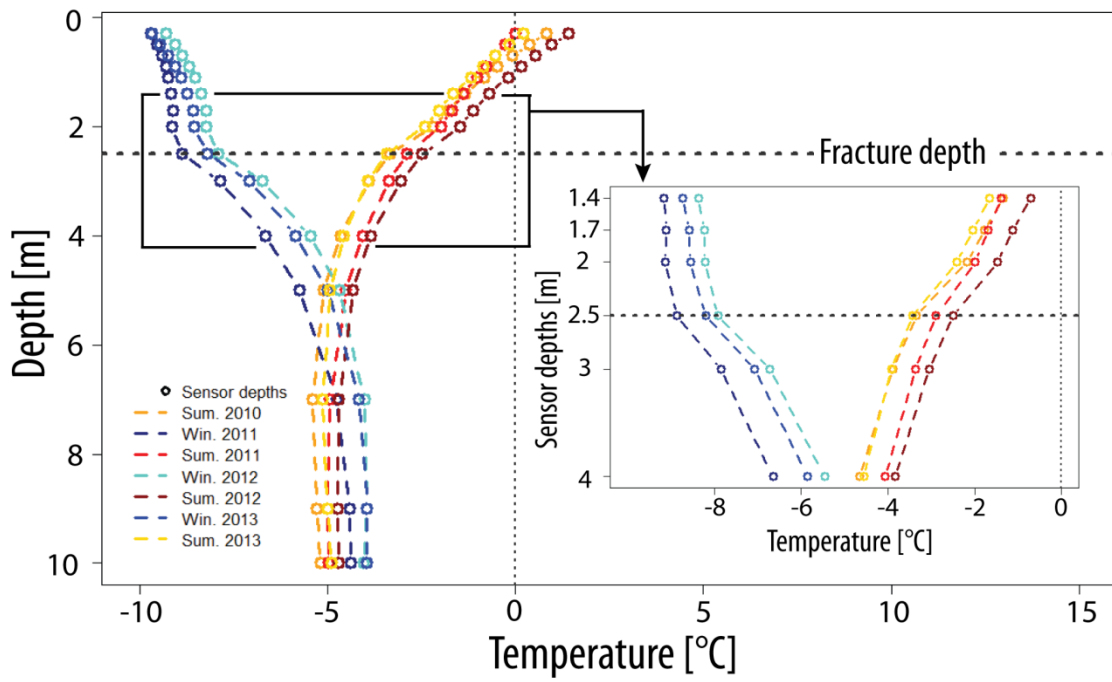
850 **Figure 6.** Daily temperature records in the AdM boreholes from December 2009 to December
 851 2013.

852



853

854 **Figure 7.** Mean $T(z)$ profiles (A) and 2011 temperature envelopes (B) of the AdM boreholes.



855

856 **Figure 8.** Seasonal $T(z)$ profiles for winters (December to February) and summers (June to
 857 August) recorded in BH_N.